Polymer Journal, Vol. 39, No. 12, pp. 1207–1220 (2007)

SPECIAL ISSUES -PROGRESS IN STRUCTURE ANALYSES OF POLYMERIC MATERIALS BY SYNCHROTRON RADIATION AND NEUTRON BEAM- REVIEW ARTICLE

Strain-Induced Crystallization of Crosslinked Natural Rubber As Revealed by X-ray Diffraction Using Synchrotron Radiation

Masatoshi TOSAKA†

Institute for Chemical Research, Kyoto University, Gokasho, Uji 611-0011, Japan

(Received May 25, 2007; Accepted September 1, 2007; Published October 23, 2007)

ABSTRACT: Strain-induced crystallization (SIC) of natural rubber (NR) has been extensively studied even before the advent of macromolecular physics. However, there are still some unsolved basic issues in this field. In this review article, classic studies on SIC of NR are briefly introduced, and then recent results by synchrotron X-ray diffraction studies in separate papers by different authors are categorized and interpreted on the basis of molecular models. Cyclic deformation experiments provided information on partial orientation of the network-chains, on nucleation and morphological changes of crystals and on stress field around the strain-induced crystals. On the other hand, experiments under constant strain provided information on kinetics of SIC, on stress relaxation due to SIC, and so on. The experimental results could be explained under the assumption that the SIC is dominated by strain, and that the crystals are of folded-chain type. However, in order to consistently explain the various experimental results, we have to establish a unified molecular model of the network structure. [doi:10.1295/polymj.PJ2007059]

KEY WORDS Network-chain Density / Crosslinking / Supercooling / Entropy / Rubber Elasticity / Crystallite Size / Entanglement /

Natural rubber (NR) from *Hevea* latex is an indispensable material for many industrial and household applications,[1] which is constituted of *cis*-1,4-polyisoprene (*ca.* 94%) and non-rubber components such as proteins (*ca.* 2%) and lipid (*ca.* 3%).[2] The versatility of the plant-derived NR is mainly due to its outstanding tensile properties and the good crack growth resistance. We still cannot reproduce the good performance of the NR products using synthetic *cis*-1,4-polyisoprene rubber (IR). The superiority of NR has been thought to originate from its ability to crystallize immediately by expansion; by contrast, crystallinity of IR is not as high as NR because of the lower regularity of the main-chain structure.[2,3] In this context, strain-induced crystallization (SIC) of NR has been extensively studied even before the advent of macromolecular physics.[4]

In spite of the long history of the study, there are still some unsolved basic issues in this field. The principal problem is the lack of widely-accepted framework to understand this phenomenon. Even the basic morphological features, *e.g.*, existence of chain folding or the physical crosslinking by the strain-induced crystallites, are still discussed. From the thermodynamic viewpoint, some researchers regard the primary factor of this type of crystallization to be stress, and hence they use the term "stress-induced crystallization."[5] By contrast, others (including the author of this article) regard strain to be the primary factor, using the term "strain-induced crystallization." We have to establish a common basis on which various experimental evidences, including the mechanical and morphological features along with the thermodynamic properties, are consistently understood. This review article is written on the basis of a framework which I believe to be fair. Nevertheless, the framework may have to be corrected to explain the rest of unsolved issues. In this article, at first, classic studies on SIC of NR are briefly presented, and then recent synchrotron X-ray diffraction studies are summarized along with discussions on some unsolved issues.

CLASSIC STUDIES ON SIC OF NR

Experimental studies

The wide angle X-ray diffraction (WAXD) pattern of stretched NR sample has been already reported in 1925 by Katz.[6] (Note that commercially important synthetic polymers were introduced after 1930's, which include poly(vinyl chloride), poly(methyl methacrylate) and polystyrene.[7]) He recognized that the isotropic amorphous halo remains in the WAXD pattern of crosslinked NR even when the sample is stretched up to 500% of the original length and that the fiber-pattern-like crystalline reflections appear

†To whom correspondence should be addressed (Tel: +81-774-38-3062, Fax: +81-774-38-3069, E-mail: tosaka@scl.kyoto-u.ac.jp).

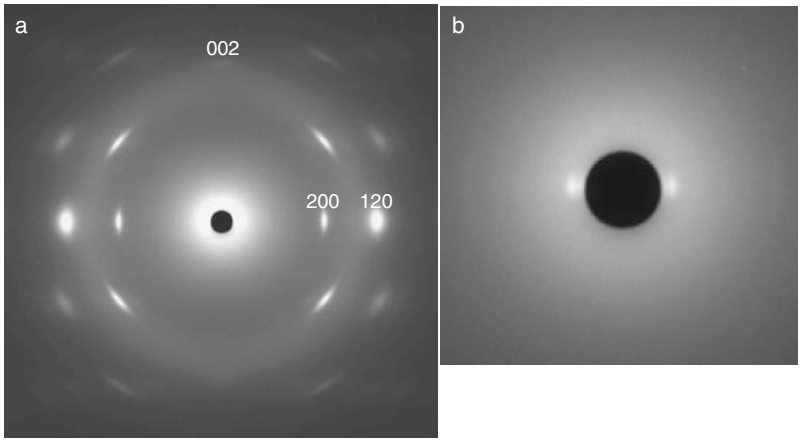

Figure 1. Typical WAXD pattern from a stretched sample of crosslinked NR. Indices of major reflections are indicated in part a. Part b is the enlargement of the central area in part a, which shows the reflections from stearic acid crystals near the beamstop.

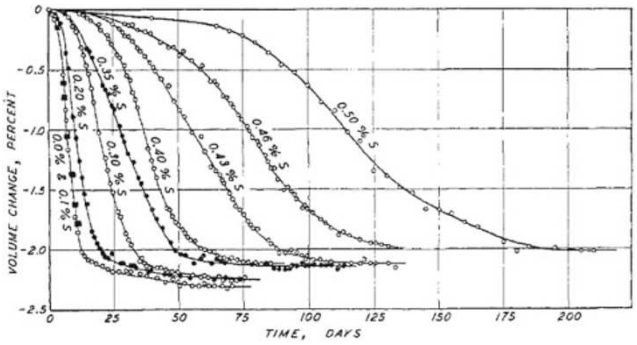

Figure 2. Volume change of sulfur-crosslinked NR with time at 2 °C. Reprinted with permission from *Ind. Eng. Chem.*, **33** (3), 381–384 (1941). Copyright 1941 American Chemical Society.

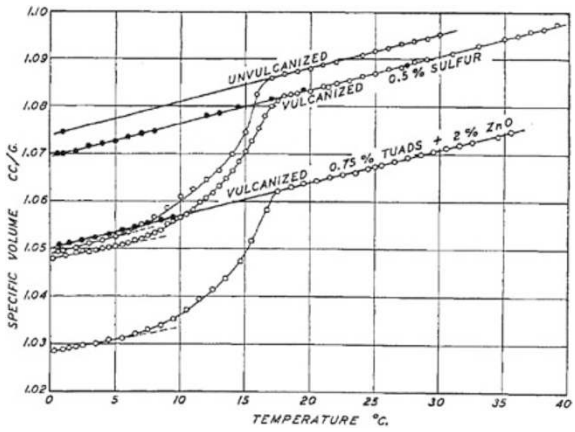

Figure 3. Specific volume of NR as a function of temperature. The open circles represent observations during the first heating following crystallization at 2 °C; the dark circles, during subsequent heating. These two sets of plots converge as a result of crystal melting. The temperature range of melting is not affected by the amount of crosslinking agent. Reprinted with permission from *Ind. Eng. Chem.*, **33** (3), 381–384 (1941). Copyright 1941 American Chemical Society.

near the halo ring. Figure 1a shows the typical WAXD pattern from a highly stretched sample of NR. The peculiarity of this feature in contrast to the WAXD patterns from other semicrystalline polymer materials has been discussed by Clark *et al.* in 1941.[8] However, they could not give any molecular theory to explain the peculiar feature; there were not enough knowledge, theories and experimental techniques to deeply analyze this issue in those days.

It was indeed in 1941 when the pioneering works on crystallization kinetics of NR by Bekkedahl & Wood was just published.[9] They applied dilatometry (namely, volume measurements) to monitor the development of crystallization. In this work, two important features on the crystallization of unstretched samples of crosslinked NR were presented. One is that the rate of crystallization decreases with the increase in the amount of crosslinking agent (namely, sulfur), as shown in Figure 2. The other is that, when the crosslinked NR samples are crystallized at a certain low temperature, the melting temperature is independent of the amount of sulfur (Figure 3). Their subsequent work[10] in 1946 has been cited in major textbooks on polymer physics as a typical example showing the dependence of polymer crystallization rate on temperature; in the case of NR, the crystallization rate showed a maximum at *ca.* −25 °C.

The kinetics of crystallization in stretched sample, namely SIC, of crosslinked NR was reported by Gent[11] in 1954. The experimental time ranged from a few to over 10^5 min (*ca.* 3 months). He showed that SIC is accelerated with the increase in strain, while it is slowed down with the increase in crosslinking density. The Avrami analysis was extended to polymer crystallization considering the fraction of uncrystallizable polymer molecules; the Avrami exponent was found to vary from 3 (*e.g.*, spherical growth) for unstretched sample to 1 (*e.g.*, needle-like growth) for highly stretched one. Along with the volume change, he measured stress relaxation due to SIC, which had been predicted by Flory.[12]

Much faster kinetics of SIC was studied by Mitchell & Meier[13] in 1968 on the basis of thermal measurements. They quickly stretched the crosslinked NR sample to a predetermined strain ratio, and measured the excess temperature rise due to SIC. The estimated time constant of SIC was around 50 ms.

The crystal structure of NR considering statistical replacement of equivalent molecular chains with mirror symmetry was proposed by Nyburg[14] in 1954. This structure was approved by Natta & Corradini,[15] and has been regarded to be the probable one as yet. (In terms of the discrepancy factor, this crystal structure is not so good and is not necessarily acceptable at present. Recently, Takahashi & Kumano[16] refined the crystal structure of NR using modern techniques. The statistical structure has been approved also in their work.)

The equilibrium melting temperature of *cis*-1,4-polyisoprene crystal was estimated by Dalal *et al.*[17] to be *ca.* 35 °C using IR as the sample.

A quantitative WAXD study on SIC of crosslinked NR was presented by Mitchell in 1984.[18] He also recognized the persistence of the isotropic halo. By utilizing this feature, he proposed a simple method for the evaluation of crystalline fraction: By measuring the decrease in intensity (after correction for the sample thickness) at a fixed part of the halo, the fraction of the crystal phase was estimated. This method has been adopted by several other researchers.

In terms of polymer crystallization, chain folding is an important issue. Though Keller's finding of chain folding[19] in 1957 for solution-grown single crystals of polyethylene has been widely accepted, the first experimental evidence on chain folding had been reported in 1938 by Storks.[20] He crystallized thin film of gutta-percha which is an isomer of NR (*i.e.*, gutta-percha is *trans*-1,4-polyisoprene). Electron diffraction patterns evidenced that the molecular chains aligned perpendicular to the film surface, which consequently require the chain folding. Now, for the NR samples without crosslinking, direct evidences for the growth of folded-chain lamellar crystals have been obtained by transmission electron microscopy.[21–24] On the other hand, experimental reports on the growth of lamellar crystal for crosslinked NR samples are quite limited. Probably, informative results have not been obtained at room temperature by the small-angle X-ray scattering experiments of the crosslinked samples. One of the limited exceptions is the report by Luch *et al.*,[25] in which the two-spot pattern suggesting the lamellar morphology was observed at low temperature. However, the two-spot pattern disappeared as the sample temperature was elevated to room temperature, though the SIC was confirmed by the WAXD pattern at room temperature. Accordingly, the report by Luch *et al.*[25] does not necessarily indicate that the strain-induced crystals always accompany the chain folding.

Theoretical studies

The crystallization theory of stretched polymer network was proposed by Flory[12] in 1947. By assuming a uniform network structure and the equilibrium state, he formulated, *e.g.*, the degree of crystallization as a function of strain ratio (α) and temperature. (In this article, the strain ratio, α, is defined as l/l_1; l and l_1 are the length of the deformed and the initial states of the sample, respectively.) The incipient crystallization temperature of stretched polymer network ($T_{i,\alpha}$) was formulated as;

$$\frac{1}{T_{i,\alpha}} = \frac{1}{T_{i,1}} - \frac{R}{\Delta H}\psi(\alpha, n), \tag{1}$$

where $T_{i,1}$ is the incipient crystallization temperature of unstretched sample, R is the gas constant, ΔH is the heat of fusion, and n is statistical number of segments in the network chain. $\psi(\alpha, n)$ has the form;

$$\psi(\alpha, n) = \left(\frac{6}{\pi}\right)^{\frac{1}{2}}\left(\frac{\alpha}{n^{\frac{1}{2}}}\right) - \left(\frac{\alpha^2}{2} + \frac{1}{\alpha}\right)\cdot\frac{1}{n}. \tag{2}$$

Equations 1 and 2 suggest that T_i changes with the length of network chain, in other words, with the network-chain density (ν). He predicted that stress relaxation will occur as a result of SIC, because the molecular chains in the crystallites adopt the extended conformation aligned in the stretching direction and the remaining amorphous portion is relaxed.

Thereafter, several other theories on SIC of crosslinked rubber have been proposed. According to Yamamoto & White,[26] occurrence of SIC in the crosslinked rubber is explained as follows. When the amorphous sample is expanded, the network chains become oriented in the stretching direction and their end-to-end distances are increased. The orientation, stretching, and thus partial ordering of the polymer chains decreases the configurational entropy of the sample by an amount ΔS_{def} and thus decrease the entropy change of fusion. The melting temperatures (T_m) of unstretched and stretched samples are given by the following equations,

$$T_{m,1} = \frac{\Delta H_1}{\Delta S_1} \tag{3}$$

$$T_{m,\alpha} = \frac{\Delta H_\alpha}{\Delta S_\alpha} \tag{4}$$

where ΔH and ΔS are the heat of fusion and entropy of fusion, respectively, at the strain ratio designated by the subscripts. The T_m in the stretched state will be elevated by an amount

$$T_{m,\alpha} - T_{m,1} = \frac{\Delta H_\alpha}{\Delta S_\alpha} - \frac{\Delta H_1}{\Delta S_1}. \quad (5)$$

If the heat of fusion is independent of the deformation ($\Delta H_1 = \Delta H_\alpha$), Equation 5 will be rewritten as

$$\frac{1}{T_{m,\alpha}} = \frac{1}{T_{m,1}} + \frac{\Delta S_{def}}{\Delta H_1}, \quad (6)$$

where $\Delta S_{def} = \Delta S_\alpha - \Delta S_1$. When T_m exceeds the ambient temperature and attains sufficient supercooling, SIC will take place. On the basis of this idea, they described the incipient crystallization temperature in a different form from the Flory's one. The exact description of the formulation is found in the original literature.[26]

While these theoretical studies assumed homogeneous deformation, another school of theory assumed inhomogeneous deformation of network chains. For example, Tonelli & Helfand[27] discussed the existence of loops and dangling chains in the network, which are elastically ineffective. The fraction of the elastically ineffective chains was estimated to be 10–20%. Similarly, Dietrich *et al.*[28] considered the influence of finite extensibility of the network-chains in the stretched samples. They concluded that, in the stretched network having the distribution of network-chain length, the proportion of fully extended chains is small, while other "relaxed" chains are only slightly oriented. Reichert *et al.*[29] extended this idea to the SIC of filled elastomer, assuming that the volume fraction of fully extended chains is proportional to the fraction of strain-induced crystals. Though the latter assumption does not explain the observed crystallization behavior, the characteristic feature in the WAXD pattern reported by Kats,[6] Clark *et al.*[8] and Mitchell[18] (see Figure 1a) appears to be consistent with this school of theory.

CYCLIC DEFORMATION

Dichotomization of molecular chains and nucleation

By using a conventional X-ray source, single exposure for acquisition of a meaningful two-dimensional WAXD pattern takes, at least, several minutes. Thanks to the powerful synchrotron X-ray source, WAXD measurement of crosslinked NR samples under cyclic deformation became less time-consuming. The peculiar feature in the WAXD pattern, namely the coexistence of the highly oriented crystalline reflections and isotropic amorphous halo, was quantitatively analyzed by Murakami *et al.*[30] and Toki *et al.*[31] In these two works, crosslinked NR samples having the same composition were studied. A tabletop stretching machine was placed on the beamline in SPring-8, Japan or National Synchrotron Light Source (NSLS), USA. In this case, tensile stress was simultaneously measured during the acquisition of the WAXD patterns. The simple method by Mitchell[18] for the estimation of crystallinity was not adopted, because it ignores the existence of oriented amorphous fraction. They indeed estimated the fraction of oriented amorphous separately. By analyzing the stress values along with fractions of crystal, isotropic and oriented amorphous phases, they clarified that most chains remain in the isotropic amorphous phase, even when crosslinked NR is highly stretched; only a few percent of the amorphous chains are oriented and the rest of the chains are in the crystal phase. Thus they suggested the importance of strain-induced crystals on the mechanical properties of NR. The similar analysis was applied to other synthetic rubber materials, and the dichotomization to the highly oriented crystal and the unoriented amorphous phases was confirmed also for the different types of rubber materials.[32–35]

According to Tosaka *et al.*,[36] another highly oriented component exists in a stretched sample even before the emergence of NR crystals; they noticed that highly oriented reflections of stearic acid (SA) crystals (Figure 1b) are observed before the emergence of reflections from NR crystals. Now, it is well known that, in the case of unstretched NR, SA acts as nucleating agent which drastically accelerates crystallization at low temperature.[2,37,38] Though SA could work as the nucleating agent, Tosaka *et al.* supposed that the highly oriented network chains do initiate SIC. A later study by Kohjiya *et al.*[39] evidenced that, in the case of SIC, the nucleating effect of SA is negligible. Even in the IR sample which was totally free from SA, SIC proceeded without any retardation. On the contrary, acceleration of SIC was not observed by mixing SA in IR.

Incipient strain of crystallization

Tosaka *et al.*[36,40] studied SIC of crosslinked NR and IR samples having various ν values at NSLS. The other important features of SIC of crosslinked NR were presented in these works. They noticed that the incipient strain of crystallization (α_i) was almost independent of ν. By contrast, α_i was definitely different between the NR and IR samples; the α_i of IR samples was the larger (Figure 4; in this article, the larger number in the sample code indicates the smaller ν). Toki *et al.*[41] and Trabelsi *et al.*[42] also showed that IR require the larger strain than NR to start SIC. According to Equation 6, the shift of α_i between NR and IR samples should be attributed to the difference in T_m of unstretched samples, namely $T_{m,1}$. Because $T_{m,\alpha}$ must be elevated above ambient temperature from the lower $T_{m,1}$, the larger ΔS_{def}, and hence α, are required for IR to start SIC. The lower $T_{m,1}$ is

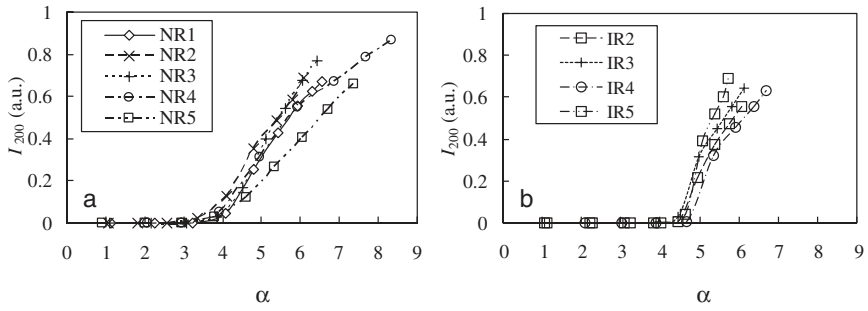

Figure 4. Crystallization behavior of (a) NR and (b) IR samples during the stretching process. The WAXD results in ref 40 were newly processed. The integrated intensity of 200 reflection (I_{200}) was normalized using the total intensity of the diffraction pattern. The smaller number in the sample code corresponds to the higher ν.

due to the lower regularity in the main-chain structure of IR.[2,3] The higher T_m of NR, not only in unstretched but also in stretched states, has been experimentally confirmed by Gent *et al.*,[43] and recently by Trabelsi *et al.*[42]

Poompradub *et al.*[44] further discussed this feature on the basis of the synchrotron WAXD studies for filled NR samples. They reported that the α_i values were also independent of the filler content, if the effective strain ratio of deformable rubber portion was taken into account. Furthermore, they found that former studies also reported implicitly that the α_i values do not depend on ν. For example, Smith *et al.*[45] measured T_i values of three types of samples having different ν. By plotting the data of α_i *vs.* crystallization temperature in ref 45, Poompradub *et al.* showed the three curves for their samples were almost superposed with each other. Other synchrotron WAXD studies by Trabelsi *et al.*[46] and Chenal *et al.*[47] also reported that samples having different ν started SIC at almost constant strain ratio. These works suggest that the strain ratio α_i for the onset of crystallization is a function of strain rate and temperature and not of ν. However, there is a difficult problem for understanding this feature.

According to Yamamoto & White[26] (Equation 6), by formulating ΔS_{def}, we can predict the behavior of T_m. Here we remember that ΔS_{def} is the entropy change due to expansion, which is the origin of the entropic elasticity of crosslinked rubber. For example, the simplest expression of ΔS_{def} assuming the Gaussian chains has been formulated in the statistical theory of rubber elasticity as;[48]

$$\Delta S_{def} = -(1/2)\nu k(\alpha_1{}^2 + \alpha_2{}^2 + \alpha_3{}^2 - 3), \quad (7)$$

where k is the Boltzmann constant and α is the strain ratio in the direction designated by the subscripts. Using equation 7, we can qualitatively reproduce the empirical features of the rubber elasticity; *e.g.*, a sample having the higher ν shows the higher modulus. Of course, there are modified expressions for ΔS_{def} considering, *e.g.*, the finite length of network chains or effect of chain entanglements. In any case, ΔS_{def} must depend on ν as evidenced by the features of the entropic elasticity. The combination of Equations 6 and 7 predicts that T_m increases with the increase in ν and α. If we assume a certain degree of supercooling as the necessary condition for SIC, the incipient strain of crystallization, α_i, should decrease with the increase in ν. The same conclusion is drawn from the Flory's theory[12] (Equations 1 and 2).

The experimental results on SIC[36,40,44–47] were not consistent with the above expectation; α_i was almost independent of ν. (The only exception may be the one for NR samples crosslinked with dicumyl peroxide.[49] In this case, the nature of the network structure could be different from the other samples crosslinked by sulfur. Otherwise, the kinetics of crystallization could have influenced because of the relatively high deformation rate adopted for this experiment.)

Now, we have to confirm that the discrepancy in question was not the consequence of experimental errors or inappropriate analysis. First, we have to check if the difference in α_i would be large enough to be detectable. Table I shows the estimated T_m on the basis of Equations 6 and 7 for the samples in ref 36 and ref 40. Here, the values of $\Delta H_1 = 25.1$ J·cm^3 (Burfield & Tanaka[3]) and $T_{m,1} = 308$ K (Dalal *et al.*[17]) were used. At room temperature, SIC started at $\alpha \approx 3$. For NR1 at this strain ratio, T_m is calculated to be 344 K, which is a reasonable value considering the supercooling. To attain the same T_m for NR5, the sample must be stretched up to $\alpha = 4.45$. Such a big difference in α_i would have been detectable.

Table I. Estimation of melting temperature for samples with different ν

Sample	Network-chain density ν (mol/cm^3)	Melting temperature $T_{m,\alpha}$ (K) $\alpha = 3$	$\alpha = 4.45$
NR1	2.12×10^{-4}	344	394
NR5	1.01×10^{-4}	324	344

Second, we have to consider the kinetics of SIC. According to Gent[11] and Trabelsi *et al.*,[46] rate of SIC is slower for the samples with the higher ν. Due to the slower crystallization, the smaller α_i for the higher ν could have compensated. If so, the observed α_i could apparently show a constant value. However, our recent studies[50,51] presented that the initial rate of SIC is faster for the samples with the higher ν. Then the predicted dependence of α_i on ν would appear more strongly, if the kinetics has really affected.

As the third point, the chain entanglements should be taken into account. The number of monomer units between the chemical crosslinkings is 100–400 for the studied samples.[36,40,45–47] On the other hand, there are only 45–100 monomer units between the physical entanglements.[52,53] Then one may suppose that the difference in ν among the samples would be obscured by the effect of entanglements, leading to the observed independence of α_i. However, the values of ν estimated from the tensile modulus[36,46] should have already counted the effect of entanglements, because the tensile modulus is related to effective number of crosslinking (including the chemical crosslinking and the physical entanglements). If the difference in ν were obscured by the entanglement, the difference not only in α_i but also in tensile modulus would not have been manifested.

In this way, the discrepancy between the theoretical prediction and experimental results concerning α_i appears to be a substantial problem.

Morphological features

Trabelsi *et al.*[46] reported by synchrotron WAXD experiments on morphological changes during the cyclic deformation of NR. They placed a tabletop stretching machine on the beamline in LURE, France; the stretching axis was tilted so that the 002 reflection came into the diffraction condition. The 002 reflection was used to estimate the crystallite size in the *c*-axis (molecular-chain) direction (namely L_{002}). During the stretching process, L_{002} decreased monotonically. When the retraction process started, L_{002} slightly increased in the beginning and then decreased. The overall changes of L_{002} were moderate, so that they regarded it to be constant. The sample with the higher ν showed the smaller L_{002} value. The degree of crystal orientation changed also moderately during the stretching process, while the orientational fluctuation gradually increased during the retracting process as the original length was recovered. We could find that the sample with the larger ν showed the smaller orientational fluctuation.

Tosaka *et al.*[36] estimated the crystallite size in the direction perpendicular to the *c*-axis (namely L_{200} and L_{120}), along with the orientation function, for NR samples with various ν values. The changes of the crystallite sizes are shown in Figure 5. During the stretching process, L_{200} and L_{120} decreased monotonically with increasing strain ratio, α. On the other hand, during the retracting process, the crystallite sizes increased in the beginning, and then decreased. Both L_{200} and L_{120} were smaller for the samples having the larger ν, and their overall changes were moderate. As for orientational fluctuation (Figure 6), the same trend found in Trabelsi *et al.*[46] was reported.

In this way, though the crystallographic directions were different, Trabelsi *et al.*[46] and Tosaka *et al.*[36] reported the same trend for the morphological changes of the strain-induced crystals in the unfilled NR samples during the cyclic deformation. By contrast, Chenal *et al.*[47] reported the slight increase in L_{200} and L_{120} with increasing strain ratio. For filled samples, changes in L_{200} and L_{120} were reported by Poompradub *et al.*[44] If we regard filler particles as large crosslinking points, the observed trend can be understood to be the same with Tosaka *et al.*[36] Interestingly, in the case of the filled samples, the crystallinity index increased when the retracting process started, and subsequently decreased after a maximum (Figure 7). The same phenomenon concerning crystallinity was reported by Toki *et al.*[54] also for unfilled samples.

These behaviors observed for crystallite size (except for the results by Chenal *et al.*[47]), orientation function and crystallinity during the cyclic deformation would be consistently explained as follows. Let us consider the stretching process first. In general, the higher nucleation density leads to the smaller crystals. With the macroscopic expansion of the sample, the number of stretched chains that can act as nuclei must increase. Then the increase in nucleus density with expansion of the sample would result in the smaller lateral crystallite size (L_{200} and L_{120}). The larger ν value should also lead to the higher nucleus density, and hence, the smaller lateral crystallite size will result (Figure 5). On the other hand, the longitudinal crystallite size (L_{002}, namely the lamellar thickness) may be determined by the average network-chain length and supercooling. (It is known that the lamellar thickness is the smaller when the supercooling is the larger, for the quiescent crystallization of linear polymer.[55]) With the increase in the strain ratio α, melting temperature T_m (Equation 6) and hence supercooling would increase. As a result, L_{002} may moderately decrease with α. The fluctuation of crystalline orientation (Figure 6) can be related to the lateral crystallite size, considering the twisting of chain-folded lamellar crystals. The twisting, probably due to the existence of chain folding on the surface, is known for many polymer species.[56] The twisting is related to the

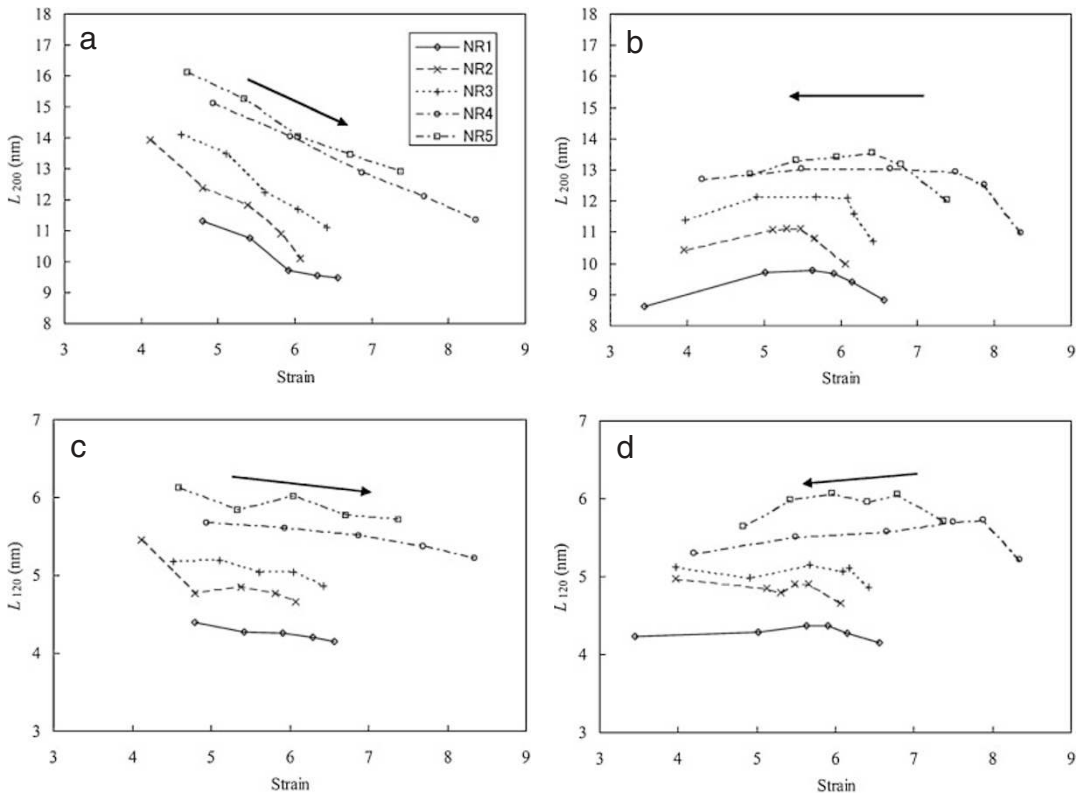

Figure 5. Lateral crystallite size as a function of strain ratio; for L_{200}, (a) during the stretching process, (b) during the retracting process, and for L_{120}, (c) during the stretching process, and (d) during the retracting process. The smaller number in the sample code corresponds to the higher ν. Reprinted with permission from *Macromolecules*, **37**(9), 3299–3309 (2004). Copyright 2004 American Chemical Society.

undulation of chain axis in the crystallites.[57,58] Because of the twisting of lamellar crystals, the larger crystallites in the NR sample with the smaller ν may have shown the higher degree of orientational fluctuation (Figure 8).

The crystallites should locate along the relatively short and tightly stretched trajectories in the network. Accordingly, the mobility of crystallites and the stretched chains should be considerably restricted, unless the tension is released. During the stretching process, some of the stretched chains may remain in oriented amorphous state, if there are no other stretched chains in the neighborhood to form a crystallite with them. At the beginning of the retracting process, such crystallites and the stretched chains may retrieve mobility, and reorganize to form the larger crystallites through partial melting (Figure 5b and 5d). In some cases, crystallinity may increase by incorporating the oriented amorphous chains, as in Figure 7. With the further progress of the retracting process, however, the crystallites would gradually melt and the relaxation of the network would increase the orientational fluctuation (Figure 6b).

Stress field around the crystals

For unfilled NR samples, the relationship between the lattice constants of the unit cell and the nominal tensile stress was studied.[36] The unit cell of the NR crystallites was elongated along the *c*-direction while it shrunk along the *a*- and *b*-directions, almost linearly with the tensile stress. Such a linear deformation of crystal lattice in relation to stress cannot be explained by a typical mechanical model which is composed of serial and parallel connections of crystallites (Figure 9a). Because the fraction of crystals changes with the strain ratio and the tensile stress, the number of crystals in Figure 9a (illustrated as the boxes) must also change. Then the relationship between the deformation of each crystallite and the nominal stress would depart from the linearity. In order to explain the observed result, other type of mechanism such as the transfer of hydrostatic stress must be considered. Thus Tosaka *et al.*[36] proposed the mechanical model in which the crystals are surrounded by the framework of network chains (Figure 9b).

The same analysis was applied for filled samples.[44,59] In this case, again, lattice constants changed linearly with the tensile stress. It is noted that, for unfilled NR, the slopes of the stress *vs.* lattice constant plots were identical among the samples having different ν values.[36] By contrast, the slopes became the more gradual with increasing filler content, as in Figure 10.[44] This result was explained by the model in Figure 9c, assuming that some of the filler particles

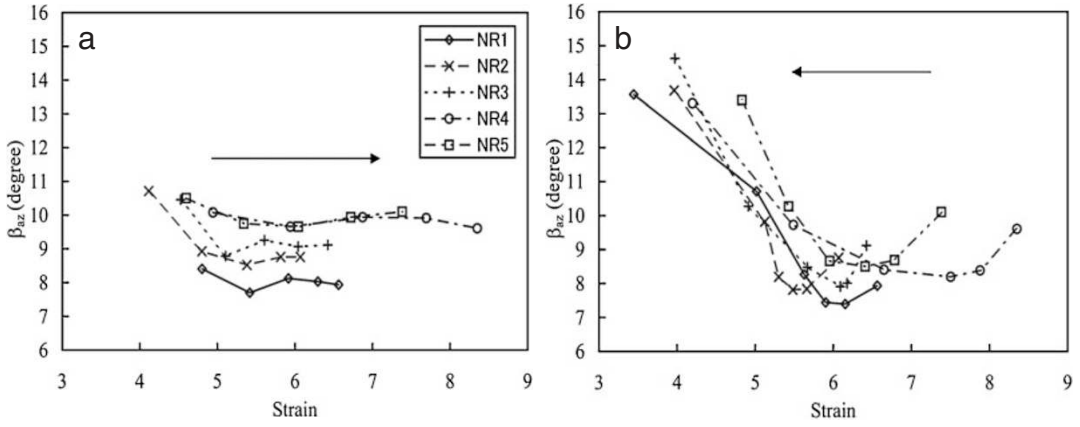

Figure 6. Azimuthal half-width of the 200 reflection as a function of strain ratio during (a) the stretching process and (b) the retracting process, respectively. The smaller number in the sample code corresponds to the higher ν. Reprinted with permission from *Macromolecules*, **37**(9), 3299–3309 (2004). Copyright 2004 American Chemical Society.

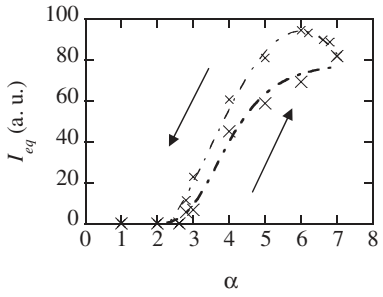

Figure 7. Integrated intensity of the equatorial reflections as a function of strain ratio for NR containing 13.5 vol % of calcium carbonate. Thick and thin lines indicate the stretching and the retracting processes, respectively. The larger symbols correspond to the stretching process. Reproduced from *J. Appl. Phys.*, **97** (10), 103529 (2005), Copyright 2005, American Institute of Physics.

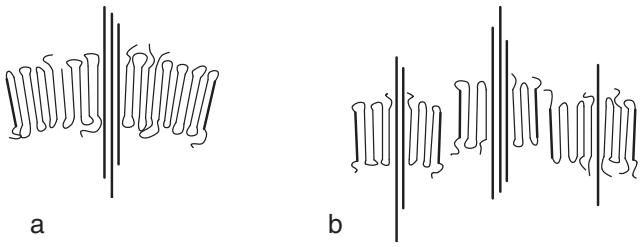

Figure 8. Orientational fluctuations of crystallites due to bending of lamellae. Thick lines in the center of each crystallite represent nuclei. Direction of thick lines on both sides of crystallites should be compared. Degree of fluctuations in the larger crystallite in part a is larger than that in smaller crystallites in part b.

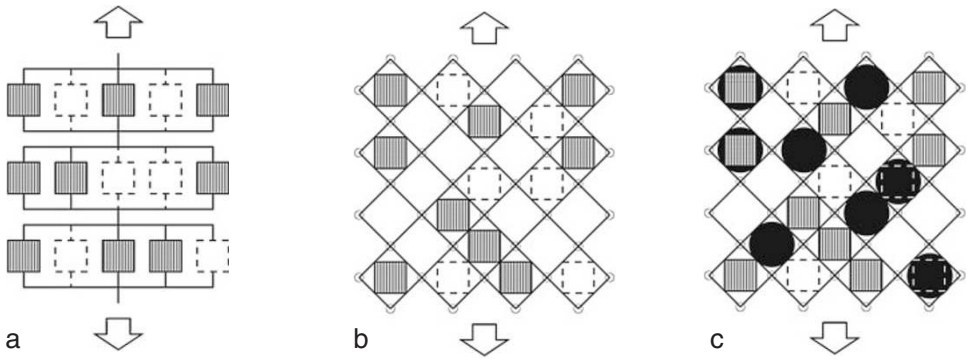

Figure 9. Mechanical models to explain the deformation of NR crystallites. Striped squares indicate existing crystallites. Additional crystallites will be formed during deformation as illustrated by broken lines. (a) Combination of serial and parallel connections of crystallites. (b) Crystallites are located between the frames with the flexible connectors. The external force is transferred to the crystallites like the hydrostatic pressure. (c) Same as part b but some of the filler particles (illustrated by the filled circles) occupy the same cell with the crystallites. On average, less stress is apportioned to the NR crystallites.

share the same "cell" with the NR crystals. It should be noted that the models in Figure 9b and 9c are highly simplified, ignoring the morphological feature that the strain-induced crystals would be formed on the stretched network chains. Establishment of more detailed model is necessary for exact understanding.

In the case of filled NR, reduction of tensile stress after the first deformation cycle (so called Mullins ef-

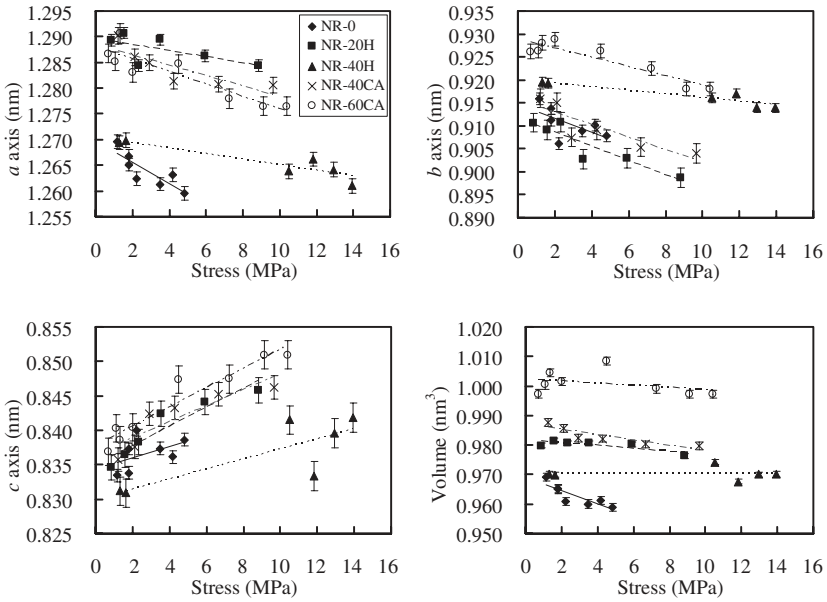

Figure 10. Lattice constants and volume of the unit cell as a function of nominal stress. Both the stretching and retracting processes are included in the plots. The numbers in the sample code designate the amount of filler (parts per hundred parts of rubber), and the symbols H and CA designate HAF carbon black and calcium carbonate fillers, respectively. Reproduced from *J. Appl. Phys.*, **97** (10), 103529 (2005), Copyright 2005, American Institute of Physics.

fect[60]) is well known. By simultaneous measurements of WAXD and tensile stress, Trabelsi *et al.*[61] showed that the behavior of SIC during the cyclic deformation was almost identical regardless to the repeated number of the cycles, though the Mullins effect was clearly observed in the stress-strain curves. They did not explain this peculiarity by a molecular model. However, as the Mullins effect would be related to chain scission and the corresponding change in ν, this result may be related to the constant α_i regardless to the variation of ν.

CRYSTALLIZATION UNDER CONSTANT STRAIN

Kinetics of SIC

Besides the dynamic experiments, studies on kinetics of SIC at a fixed strain ratio are also informative. In this type of studies, a sample was expanded to a predetermined strain ratio (α_s), and the development of SIC with time was examined. In most classic studies, the stretched sample was equilibrated at elevated temperature and then quenched to predetermined crystallization temperature to start SIC.[11,62,63] Relatively slow kinetics of SIC have been studied under the condition of small α_s and in long time scales ranging from several minutes to several months, because the rate of SIC at high elongation is too fast for typical X-ray or volume measurements to follow. Probably, the only exception reporting the fast kinetics of SIC has been the thermal study by Mitchell & Meier.[13] Unfortunately, their experimental method was insensitive for the phenomenon longer than a few second, because the excess heat is dissipated in a few seconds, leading to inaccurate analysis.

Trabelsi *et al.*[46] studied the kinetics of SIC at $-25\,^{\circ}C$ by the synchrotron WAXD. The values of α_s were up to 4, and the crystallization halftime ranged between 1 to 5 min. With the progress of SIC, the tensile stress decreased as predicted by Flory.[12] SIC was accelerated with the increase in α_s. The sample with the lower ν crystallized the faster. These results are consistent with the classic experimental studies.[9,11]

Tosaka *et al.*[50,51] studied SIC and corresponding stress relaxation during the shorter time ranging *ca.* 8 s to 30 min for NR and IR samples with various ν. The samples were rapidly expanded to $\alpha_s = 6$ and kept at the length. During the crystallization process at the constant length, fast time-resolved measurements of WAXD patterns and tensile stress were carried out. Acquisition of a two-dimensional WAXD pattern was repeated in every 83 ms during the fastest time-resolved measurement. In the NR samples, SIC quickly progressed compared to the IR samples (Figure 11). In this case, the rate of SIC was the faster for the samples with the higher ν, which is the opposite trend found in the former works.[9,11,46] This fact indicates that we observe different aspect of SIC depending on the time scale of the observation. During the initial stage of SIC, the density of stretched chains acting as nuclei would be rate controlling. However, crosslinking points cannot be included in crystallites. In the latter stage of SIC, the necessity to exclude

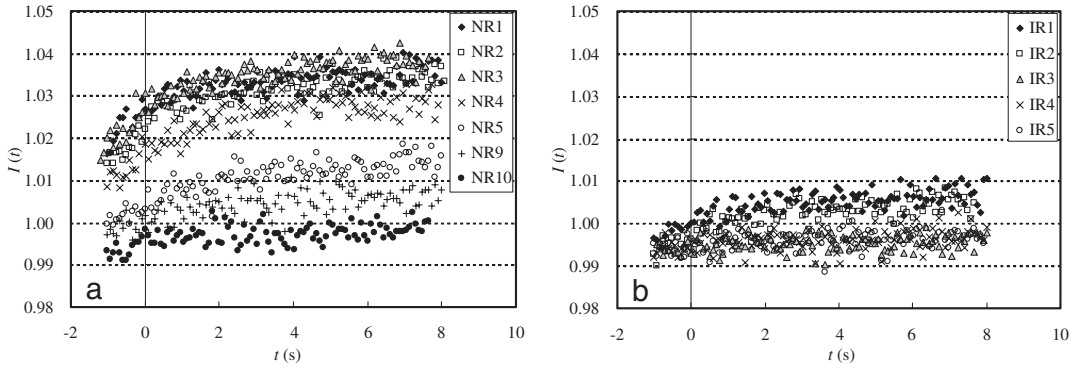

Figure 11. Crystallization behaviors in 8 s for (a) NR and (b) IR samples. $I(t)$ denotes the normalized intensity of the 200 reflection. The smaller number in the sample code corresponds to the higher ν. Reprinted with permission from *Macromolecules*, **39**(15), 5100–5105 (2006). Copyright 2006 American Chemical Society.

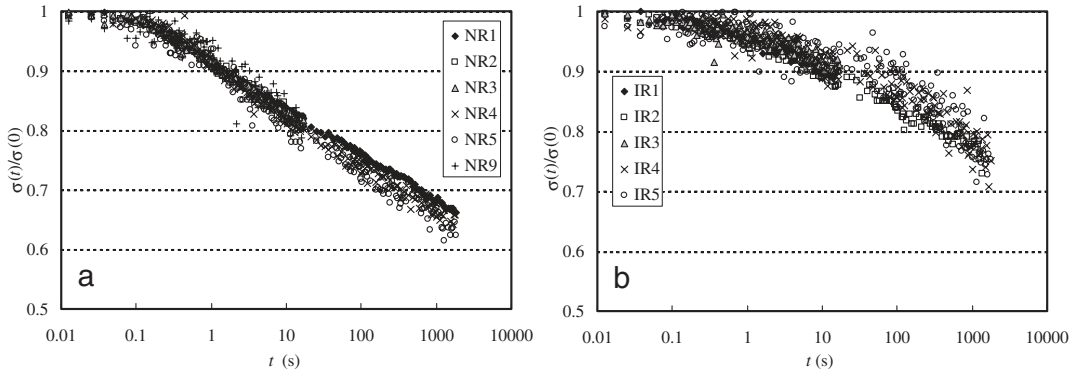

Figure 12. Tensile stress normalized by the maximum stress, $\sigma(0)$, for (a) NR and (b) IR samples. The smaller number in the sample code corresponds to the higher ν. Reprinted with permission from *Macromolecules*, **39**(15), 5100–5105 (2006). Copyright 2006 American Chemical Society.

the crosslinking from crystallizing molecular chains would retard the crystallization rate, and at the same time, would diminish the attainable crystallinity.[9,11,42] According to the new results,[50,51] we may have to reconsider the material design when we expect the reinforcing effect of SIC for quickly deformed products.

The combination analysis of WAXD and tensile stress, $\sigma(t)$, has led to the more detailed discussion on the stress relaxation due to SIC (t is elapsed time).[50,51] The measured stress relaxation reflects contributions both from SIC and from plastic deformation. By using the time constant of SIC estimated from the WAXD study, relative contributions of the two factors in the total degree of stress relaxation were separately evaluated. In the short range of time, the contribution of SIC was found to be dominant.[50] Now, the stress relaxation behavior with elapsed time after normalization by the initial (maximum) stress value, $\sigma(0)$, was almost independent of ν (Figure 12). On the other hand, the development of SIC obviously depended on ν (Figure 11). Though some of NR and IR samples showed the similar crystallization behavior, their stress-relaxation behaviors were quite different (*e.g.*, NR9 and IR2 in Figures 11 and 12). If we assume that the degree of stress relaxation is proportionally related to the mass crystallinity, this behavior cannot be explained. To explain these results,[51] we have to consider the dichotomization of the expanded network to the stretched and the loose chains. The mechanical model of the stress relaxation is schematically illustrated in Figure 13. The left side is the initial state before SIC. As time passes, the stretched chains along the short trajectories crystallize, as illustrated in the right side (crystals are drawn as rectangles). Because of the SIC, stress relaxation will occur. The loose chains (encircled by the broken lines) are assumed to be ineffective to the nominal stress. Then the nominal stress is approximated to be the sum of the retracting force exhibited by the stretched network chains along the short trajectories (drawn on the both sides of the model). The number of such short trajectories, and hence the nominal stress, are approximated to be proportional to ν. However, the stress value $\sigma(t)$ ($\propto \nu$) normalized by the initial value $\sigma(0)$ ($\propto \nu$), namely $\sigma(t)/\sigma(0)$, is independent of ν. In this case, $\sigma(t)/\sigma(0)$ reflects the stress per unit number of the

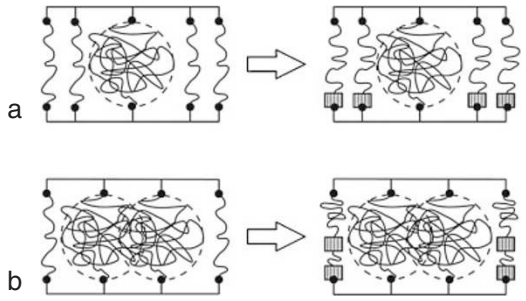

Figure 13. Schematic drawing of the stress relaxation in rubber network due to SIC. The left side is the initial state before SIC. After a certain elapsed time, strain-induced crystallites (depicted by the rectangles) are formed on the stretched chains, as shown in the right side. (a) The sample has high ν and low crystallization rate. (b) The sample has low ν and high crystallization rate. In both cases, the final amount of crystallites is the same.

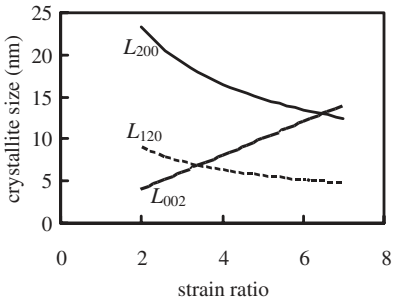

Figure 14. Illustration of the dependence of crystallite sizes L_{200}, L_{120} and L_{002} on strain ratio assuming the affine deformation.

short trajectories (which correspond to the stress per one stretched chain in Figure 13). If the rate of crystallization is the same (*e.g.*, among the NR samples) no difference is found for $\sigma(t)/\sigma(0)$, as in Figure 12. By contrast, the difference in crystallization rate between NR and IR[2,3] is exhibited in Figure 11. In Figure 13, part a shows the case for high ν and low crystallization rate (*e.g.*, IR2), while part b shows the case for low ν and high crystallization rate (*e.g.*, NR9). In both cases, the bulk crystallinity (the number of rectangles in the right side) is the same after certain elapsed time (right side). As a result, the crystallization behavior is not so different among these samples (Figure 11). This idea is basically consistent with the conclusion by Murakami *et al.*[30] and Toki *et al.*;[31] the stretched chains are responsible for the mechanical properties of crosslinked rubber, though their fraction is minor.

Tosaka *et al.*[50,51] reported the experimental results only for the case of $\alpha_s = 6$. By contrast, Toki *et al.*[64] studied SIC of IR samples at various α_s values. At high α_s, SIC proceeded considerably before the sample was expanded to the predetermined length. The increment of crystalline fraction after stopping the deformation became the larger for the smaller α_s, though stress decrease was larger for the larger α_s. These trends have been discussed in terms of the rearrangement of the network structure.

Morphological features

The lateral and longitudinal crystallite sizes (L_{120}, L_{200} and L_{002}) during SIC at fixed α_s were almost constant in spite of the increase in crystallinity.[42,46,51] This fact indicates that the increase in crystallinity is due to the increased number of crystallites whose average size is constant. The crystallite size is slightly smaller for the samples with the larger ν. According to Trabelsi *et al.*,[46] after completion of SIC, the larger α_s has led to the larger L_{002} and the smaller L_{120} and L_{200}; the manner was consistent with the affine deformation (Figure 14),

$$\begin{aligned} L_{002} &= L_{002,1} \cdot \alpha, \\ L_{200} &= L_{200,1} \cdot \alpha^{-0.5}, \\ L_{120} &= L_{120,1} \cdot \alpha^{-0.5}, \end{aligned} \tag{8}$$

where $L_{hkl,1}$ denotes the extrapolated crystallite size for $\alpha = 1$. (The clerical errors in the original paper[46] are corrected in Equation 8.) The product of these three values which is related to the final volume of crystallite was almost independent of α. The final volume changed with ν, which was the same order with the mesh size of the network. (Note that L_{120} tends to be quite smaller than L_{200} because of the statistical crystal structure of NR,[14,16] as discussed by Tosaka *et al.*[51] Accordingly, we have to be careful if we consider the volume of crystallite using L_{120}.) These results suggest that the growth of strain-induced crystallites is limited by a certain property of the network structure which deform in the affine manner. (Of course, the crystallites themselves do not deform in the affine manner.)

Trabelsi *et al.*[42] studied the distribution of the crystalline zone around crack tip. A crosslinked NR or IR sample with a notch was stretched to a predetermined strain ratio and fixed on a movable stage. By scanning the sample using the collimated beam, the crystalline zone was identified. In the case of NR, the dimension of the crystalline zone increased in the directions both parallel and perpendicular to the stretching direction with increasing the strain ratio. By contrast, the dimension of the crystalline zone perpendicular to the stretching direction was almost constant for IR. Thus the area of the crystalline zone was the smaller for IR. These results support the assumption that the reinforcing effect of strain-induced crystals is responsible for the superior crack-growth-resistance of NR to IR.

The type of strain-induced crystals in the crosslinked NR (or IR) is an important issue. If they are folded-chain (lamellar) crystals, the interpretation for the morphological changes during the cyclic deforma-

tion (in the previous chapter) is justified. However, some of the researchers assume that strain-induced crystals are of fringed-micell type. If the highly stretched chains are exclusively included into the crystals to form the fringed-micell crystals, the amount of such stretched chains would be equal before and after crystallization at a constant strain. In this case, the dense parallel packing of oriented chains before crystallization would exhibit layer lines in the WAXD pattern. Tosaka *et al.*[51] demonstrated that, by the removal of isotropic halo, such layer lines are absent in the WAXD pattern before the development of SIC. That is to say, the molecular chains that are incorporated into strain-induced crystals are not so stretched before crystallization. Though this result does not directly indicate that the strain-induced crystals are folded-chain crystals, the existence of chain folding should not be ruled out.

Now, one may wonder why we cannot observe the long-spacing of the lamellar crystals in the stretched samples of crosslinked NR at room temperature.[25] One reason may be the small lateral crystallite size of the strain-induced crystals. As mentioned above, the lateral crystallite sizes (L_{200} and L_{120}) of the strain-induced crystals do not increase with the increase in crystallinity. Discontinuous crystals may be dispersed in the stretched NR samples. In such a case, the long-spacing or the two-spot pattern may not be observed. Another reason may be the inhomogeneous and variable supercooling. As shown in Figure 13, we have to consider the degree of stretching for each network trajectory. The degree of effective supercooling expected from Equation 6 may be different for each of the trajectory. With the progress of SIC, some part of the network chain may become looser, changing supercooling with time. In this way, the supercooling is not constant in the stretched sample of crosslinked NR. Then the distribution of lamellar thickness which is dominated by supercooling would be quite large. In this case, again, the long-spacing or the two-spot pattern may not be observed.

Melting process

The melting process of strain-induced crystals of crosslinked NR is quite complicated, because it is affected not only by thermal but also by deformation histories. For example, Trabelsi *et al.*[46] studied the melting behavior of NR samples crystallized at $-25\,^{\circ}C$. The samples were heated by steps of $5\,^{\circ}C$ up to the complete melting; at each temperature, the sample was equilibrated before the WAXD measurements. On the basis of the WAXD analysis, they showed that T_m increases with increasing α and decreases with increasing ν. This appears to be contradictory to the classic work by Bekkedahl & Wood[9]

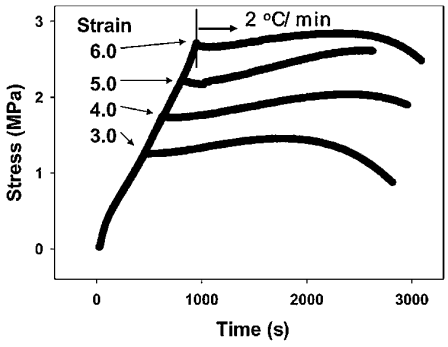

Figure 15. Stress changes during stretching at $30\,^{\circ}C$ and subsequent constrained heating. Reprinted with permission from *Macromolecules*, **38**(16), 7064–7073 (2005). Copyright 2005 American Chemical Society.

showing that T_m is independent of ν (Figure 3). Probably, the stepwise heating by Trabelsi *et al.* and the continuous heating by Bekkedahl & Wood may have lead to the different results.

The variation of tensile stress at fixed α_s values during constant cooling or heating was studied by Toki *et al.*[64] The rubber elasticity theory[48] predicts that tensile stress of stretched rubber increases with the increase in temperature and vice versa. The stress relaxation during the constant cooling experiment clearly indicated that the development of SIC further decrease the tensile stress than the prediction of the rubber elasticity theory. On the other hand, during the constant heating experiment, tensile stress increased first, and after experiencing a certain maximum, the stress decreased. The temperature corresponding to the maximum stress increased with increasing α_s (Figure 15). This behavior was explained by the combination of thermal degradation of chemical crosslinking and the effect of strain-induced crystals as physical crosslinking.

CONCLUDING REMARKS

In some of the works presented above, measured properties of strain-induced crystals are handled by simple relationships introducing "shift factor," "strain amplification factor," and so on. However, the validity of such treatments is quite doubtful, because the physical meanings of the introduced factors are not considered. In this article, the experimental results in separate papers by different authors were categorized and interpreted on the basis of the molecular models, considering their physical meanings. Unfortunately, we have not reached to a unified molecular model which can explain all the features of SIC. For example, why are the tensile modules and α_i related to ν differently, though both are related to ν through the entropy change by stretching (namely ΔS_{def})?

The answer could be found in the inhomogeneity of the stretched network. The rubber elasticity is formulated on the basis of the average values for the uniform network structure,[48] while the behavior of SIC and corresponding stress relaxation is strongly dependent on the local structure (namely, the stretched chains along the short trajectory) as illustrated in Figure 13. For further discussion, we would have to know more detail about the inhomogeneity in network structure of NR, and construct a proper mechanical model.

Acknowledgment. The author is grateful to the collaborators for their help, suggestions and discussions on this research works. Those individuals include: Prof. S. Kohjiya, Dr. S. Murakami, Dr. K. Senoo and Dr. S. Poompradub of Institute for Chemical Research, Kyoto University, Prof. Y. Ikeda of Kyoto Institute of Technology, Prof. B. S. Hsiao, Dr. S. Toki, and Dr. I. Sics of State University of New York at Stony Brook. The synchrotron WAXD experiments at the SPring-8 were performed under the approval of the Japan Synchrotron Radiation Research Institute (JASRI) (Proposal No. 2003B0664-ND1b-np, 2004A0388-ND1b-np, 2005A0425-ND1b-np).

NOTATION

I_{200}: integrated intensity of 200 reflection
k: Boltzmann constant
L_{hkl}: crystallite size in the direction perpendicular to the hkl plane
l: length of the sample
n: statistical number of segments in the network chain
R: gas constant
T_i: incipient temperature of strain-induced crystallization
T_m: melting temperature
t: elapsed time
α: strain ratio ($= l/l_0$)
α_i: incipient strain of crystallization
α_s: predetermined strain ratio at which strain-induced crystallization is performed
ΔH: heat of fusion
ΔS: entropy change of fusion
ΔS_{def}: entropy change of deformation
$\sigma(t)$: nominal tensile stress at time t
ν: network-chain density

REFERENCES

1. P. W. Allen and K. P. Jones, in "Natural Rubber Science and Technology," A. D. Roberts, Ed., Oxford University Press, Oxford, 1988.
2. Y. Tanaka, *Rubber Chem. Technol.*, **74**, 355 (2001).
3. D. R. Burfield and Y. Tanaka, *Polymer*, **28**, 907 (1987).
4. L. Mandelkern, *Rubber Chem. Technol.*, **66**, G61 (1993).
5. Y. Miyamoto, H. Yamao, and K. Sekimoto, *Macromolecules*, **36**, 6462 (2003).
6. J. R. Katz, *Naturwissenschaften*, **19**, 410 (1925).
7. J. Billmeyer and W. Fred, in "Textbook of Polymer Science," 3rd ed., Wiley-Interscience, New York, 1984.
8. G. L. Clark, R. L. LeTourneau, and J. M. Ball, *Rubber Chem. Technol.*, **14**, 546 (1941).
9. N. Bekkedahl and L. A. Wood, *Ind. Eng. Chem.*, **33**, 381 (1941).
10. L. A. Wood and N. Bekkedahl, *J. Appl. Phys.*, **17**, 362 (1946).
11. A. N. Gent, *Trans Faraday Soc.*, **50**, 521 (1954).
12. P. J. Flory, *J. Chem. Phys.*, **15**, 397 (1947).
13. J. C. Mitchell and D. J. Meier, *J. Polym. Sci., A-2*, **6**, 1689 (1968).
14. S. C. Nyburg, *Acta Crystallogr.*, **7**, 385 (1954).
15. G. Natta and P. Corradini, *Angew. Chem.*, **68**, 615 (1956).
16. Y. Takahashi and T. Kumano, *Macromolecules*, **37**, 4860 (2004).
17. E. N. Dalal, K. D. Taylor, and P. J. Philips, *Polymer*, **24**, 1623 (1983).
18. G. R. Mitchell, *Polymer*, **25**, 1562 (1984).
19. A. Keller, *Philos. Mag.*, **2**, 1171 (1957).
20. K. H. Storks, *J. Am. Chem. Soc.*, **60**, 1753 (1938).
21. E. H. Andrews, *Proc. R. Soc. London. Ser. A*, **270**, 232 (1962).
22. E. H. Andrews, *Proc. R. Soc. London. Ser. A*, **277**, 562 (1964).
23. T. Shimizu, M. Tsuji, and S. Kohjiya, *Mater. Sci. Res. Int.*, **4**, 117 (1998).
24. T. Shimizu, M. Tosaka, M. Tsuji, and S. Kohjiya, *Rubber Chem. Technol.*, **73**, 926 (2000).
25. D. Luch and G. S. Y. Yeh, *J. Macromol. Sci., Phys.*, **B7**, 121 (1973).
26. M. Yamamoto and J. L. White, *J. Polym. Sci., Part A-2*, **9**, 1399 (1971).
27. A. E. Tonelli and E. Helfand, *Macromolecules*, **7**, 59 (1974).
28. J. Dietrich, R. Ortmann, and R. Bonart, *Colloid Polym. Sci.*, **266**, 299 (1988).
29. W. F. Reichert, D. Göritz, and E. J. Duschl, *Polymer*, **34**, 1216 (1993).
30. S. Murakami, K. Senoo, S. Toki, and S. Kohjiya, *Polymer*, **43**, 2117 (2002).
31. S. Toki, I. Sics, S. Ran, L. Liu, B. S. Hsiao, S. Murakami, K. Senoo, and S. Kohjiya, *Macromolecules*, **35**, 6578 (2002).
32. S. Toki and B. S. Hsiao, *Macromolecules*, **36**, 5915 (2003).
33. S. Toki, I. Sics, B. S. Hsiao, S. Murakami, M. Tosaka, S. Poompradub, S. Kohjiya, and Y. Ikeda, *J. Polym. Sci., Part B: Polym. Phys.*, **42**, 956 (2004).
34. S. Toki, B. S. Hsiao, S. Kohjiya, M. Tosaka, A. H. Tsou, and S. Datta, *Rubber Chem. Technol.*, **79**, 460 (2006).
35. S. Toki, I. Sics, S. Ran, L. Liu, B. S. Hsiao, S. Murakami, M. Tosaka, S. Kohjiya, S. Poompradub, Y. Ikeda, and A. H. Tsou, *Rubber Chem. Technol.*, **77**, 317 (2004).
36. M. Tosaka, S. Murakami, S. Poompradub, S. Kohjiya, Y. Ikeda, S. Toki, I. Sics, and B. S. Hsiao, *Macromolecules*, **37**, 3299 (2004).

37. A. N. Gent, *Trans. Inst. Rubber Ind.*, **30**, 139 (1954).
38. S. Kawahara, N. Nishiyama, T. Kakubo, and Y. Tanaka, *Rubber Chem. Technol.*, **69**, 600 (1996).
39. S. Kohjiya, M. Tosaka, M. Furutani, Y. Ikeda, S. Toki, and B. S. Hsiao, *Polymer*, **48**, 3801 (2007).
40. M. Tosaka, S. Kohjiya, S. Murakami, S. Poompradub, Y. Ikeda, S. Toki, I. Sics, and B. S. Hsiao, *Rubber Chem. Technol.*, **77**, 711 (2004).
41. S. Toki, I. Sics, S. Ran, L. Liu, and B. S. Hsiao, *Polymer*, **44**, 6003 (2003).
42. S. Trabelsi, P.-A. Albouy, and J. Rault, *Rubber Chem. Technol.*, **77**, 303 (2004).
43. A. N. Gent, S. Kawahara, and J. Zhao, *Rubber Chem. Technol.*, **71**, 668 (1998).
44. S. Poompradub, M. Tosaka, S. Kohjiya, Y. Ikeda, S. Toki, I. Sics, and B. S. Hsiao, *J. Appl. Phys.*, **97**, 103529/1 (2005).
45. K. J. Smith Jr., A. Greene, and A. Ciferri, *Kollid-Z.*, **194**, 49 (1964).
46. S. Trabelsi, P.-A. Albouy, and J. Rault, *Macromolecules*, **36**, 7624 (2003).
47. J.-M. Chenal, L. Chazeau, L. Guy, Y. Bomal, and C. Gauthier, *Polymer*, **48**, 1042 (2007).
48. L. R. G. Treloar, in "The Physics of Rubber Elasticity, Third Edition," Clarendon Press, Oxford, 1975.
49. Y. Ikeda, Y. Yasuda, S. Makino, S. Yamamoto, M. Tosaka, K. Senoo, and S. Kohjiya, *Polymer*, **48**, 1171 (2007).
50. M. Tosaka, D. Kawakami, K. Senoo, S. Kohjiya, Y. Ikeda, S. Toki, and B. S. Hsiao, *Macromolecules*, **39**, 5100 (2006).
51. M. Tosaka, K. Senoo, S. Kohjiya, and Y. Ikeda, *J. Appl. Phys.*, **101**, 84909 (2007).
52. L. J. Fetters, D. J. Lohse, D. Richter, T. A. Witten, and A. Zirkel, *Macromolecules*, **27**, 4639 (1994).
53. J. F. Sanders, J. D. Ferry, and R. H. Valentine, *J. Polym. Sci., Part A-2*, **6**, 967 (1968).
54. S. Toki, T. Fujimaki, and M. Okuyama, *Polymer*, **41**, 5423 (2000).
55. J. D. Hoffman and R. L. Miller, *Polymer*, **38**, 3151 (1997).
56. B. Lotz and S. Z. D. Cheng, *Polymer*, **46**, 577 (2005).
57. M. Tsuji, M. Fujita, T. Shimizu, and S. Kohjiya, *Macromolecules*, **34**, 4827 (2001).
58. K. Taguchi, Y. Miyamoto, H. Miyaji, and K. Izumi, *Macromolecules*, **36**, 5208 (2003).
59. S. Poompradub, M. Tosaka, S. Kohjiya, Y. Ikeda, S. Toki, I. Sics, and B. S. Hsiao, *Chem. Lett.*, **33**, 220 (2004).
60. L. Mullins, *Rubber Chem. Technol.*, **42**, 339 (1969).
61. S. Trabelsi, P.-A. Albouy, and J. Rault, *Macromolecules*, **36**, 9093 (2003).
62. D. Luch and G. S. Y. Yeh, *J. Polym. Sci., Polym. Phys.*, **11**, 467 (1973).
63. H.-G. Kim and L. Mandelkern, *J. Polym. Sci., Part A-2*, **6**, 181 (1968).
64. S. Toki, I. Sics, B. S. Hsiao, M. Tosaka, S. Poompradub, Y. Ikeda, and S. Kohjiya, *Macromolecules*, **38**, 7064 (2005).

Masatoshi TOSAKA was born in Hiroshima Prefecture, Japan in 1964. He graduated from Faculty of Engineering, Kyoto University in 1987. He studied electron microscopy on polymer crystals in Graduate School of Engineering, Kyoto University under the supervision of Professor Ken-ichi Katayama. After completing his Master's degree in 1989, he joined Asahi Chemical Industry. In 1995, he was appointed as an Assistant Professor of Institute for Chemical Research, Kyoto University. He was granted a doctoral degree for a thesis entitled "Structural Study on Polymer Crystals by Cryogenic High-Resolution Transmission Electron Microscopy" in 2000 from Kyoto University under the supervision of Professor Shinzo Kohjiya. On leave from Kyoto University from 2001 to 2002, he studied epitaxial crystallization of polymers on oriented poly(tetrafluoroethylene) substrates under G. Kaupp at the University of Oldenburg in Germany as a Research Associate. He also served as a Visiting Researcher at Hyogo Prefectural Institute of Technology from 2002 to 2005, and as a Part-Time Lecturer at College of Science and Engineering, Ritsumeikan University from 2005 to 2006. Present research interests of Dr. Tosaka are divided into three areas: (1) Electron microscopy of polymer condensed states: (2) Strain-induced crystallization of network polymers: (3) Novel dissipative structures in nanometer scale induced by oriented polymer substrates.